High-Performance Tantalum Oxide Capacitors Fabricated by a Novel Reoxidation Scheme

SANG GI BYEON AND YONHUA TZENG, MEMBER, IEEE

Abstract—**High-performance tantalum oxide capacitors with excellent reliability have been developed by a two-step oxidation scheme. A novel anodic reoxidation process has been applied to the reactively sputter-deposited tantalum oxide films to make the densified oxide structure. The electrical and physical properties as well as the reliability of these two-step oxidized sputtered/anodized tantalum oxide films are shown to be much superior to those of conventional tantalum oxide films prepared by either anodization or sputtering alone. Capacitors made of this sputtered/anodized tantalum oxide film have greatly improved electrical properties, such as lower dissipation factors, higher breakdown fields, narrower breakdown distribution, lower leakage currents, less charge trapping, and better reliability than anodized or sputtered tantalum oxide capacitors. Tantalum oxide films prepared by the novel sputtered/anodized reoxidation process are very useful for applications to high-capacity storage capacitors in future high-density VLSI memories.**

I. Introduction

RECENT high-density MOS dynamic random-access memory (DRAM) devices with a small cell area have been accomplished by reducing the thickness of the SiO_2 storage capacitor insulator to maintain the required charge storage level. The reduction of SiO_2 insulator thickness is encountering the physical limits in future VLSI circuits. It is important to study the use of high-dielectric-constant insulators for future high-density VLSI memory devices. Among these insulators tantalum oxide film has received considerable attention for applications to VLSI memory storage capacitors [1], [2] because of its dielectric constant above 20.

However, several problems have hindered a wide use of tantalum oxide in electronic device and integrated circuit applications. One of the major problems is its low breakdown field strength accompanied by large leakage currents. The other problems include an asymmetric conduction behavior [3], which results in the very low cathodic breakdown field, and the dependence of the breakdown field on the counter electrode material [4]. There are several reasons for the inferior properties of tantalum oxide films formed by conventional oxidation methods such as sputtering [2], [5], anodization [1], [3], and thermal oxidation [6]. It has been reported that microcracks or pinholes formed in sputtered tantalum oxide films are main paths for large leakage currents [7]. A recent similar study has shown that the tantalum oxide film with the greatest number of microcracks exhibits the largest leakage current and the lowest breakdown field [8]. When sputtered tantalum oxide films are thermally annealed, microcracks are formed because of the shrinkage of the amorphous structure in the sputtered oxide during crystallization.

The main purpose of this work is to develop high-performance tantalum oxide capacitors by overcoming the existing problems in conventional tantalum oxide films using our novel reoxidation scheme. To achieve this, sputtered tantalum oxide films are reoxidized by anodic oxidation to seal the weak spots in the initial sputtered oxide films. These two-step oxidized films, designated as sputtered/anodized oxides, with thicknesses in the range of 400–1600 Å, are compared to the coventional tantalum oxide films prepared by either anodization or sputtering alone.

II. Experimental Procedure

Tantalum films with thicknesses of about 4000 Å were deposited onto thermally oxidized Si wafers by RF magnetron sputtering from a tantalum target. Tantalum oxide deposition was followed by switching the inlet gas from pure argon to a 20:80 oxygen–argon mixture. The sputtered tantalum oxide films with different thicknesses were deposited at a pressure of 4 mtorr by varying the deposition time. After depositing the tantalum oxide, the samples were completely reoxidized by anodic oxidation at room temperature in a 0.1-percent oxalic acid solution to form the sputtered/anodized tantalum oxide. A similar two-step oxidation of sputtered aluminum oxide films has previously been attempted to develop improved aluminum oxide capacitors [9]. Conventional tantalum oxide films were formed by either anodization or sputtering alone for comparison. Aluminum was then evaporated onto all three types of oxide films and top electrodes (area = 0.0085 cm^2) were patterned by the basic photolithographic process to form a Ta-Ta oxide-Al, metal–insulator–metal (MIM) capacitor, as shown in Fig. 1. An aluminum top electrode was chosen because of its good electrical conductivity. The oxide thickness was determined by ellipsometry and capacitance measurements. The electrical properties of these MIM tantalum oxide capacitors were

Manuscript received February 15, 1988; revised August 14, 1989. This work was supported in part by DNA 001-85-0183. The review of this paper was arranged by Associate Editor P. K. Ko.

The authors are with the Alabama Microelectronics Science and Technology Center, Auburn University, Auburn, AL 36849.

IEEE Log Number 8932810.

0018-9383/90/0400-0972$01.00 © 1990 IEEE

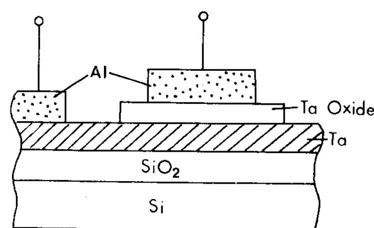

Fig. 1. Schematic of a tantalum oxide MIM capacitor.

measured using an LCR meter and an HP4145A semiconductor parameter analyzer. Physical properties of tantalum oxide films were characterized by X-ray photoelectron spectroscopy (XPS).

III. Oxide Densification

Fig. 2 shows a physical mechanism for the oxide densification attempted by our novel two-step oxidation scheme. The initial sputtered oxide has numerous weak spots such as voids, metallic particles, and thinner oxide regions, because the sputtered oxide is grown by physical impingement of tantalum and oxygen atoms. As the sputtered oxide is subjected to anodization, a higher electric field appears at the weak spots. An electric field exceeding a certain critical value causes an ionic current to flow through the weak spots, resulting in a self-sealing anodic oxidation. The self-sealing oxidation at the weak spots causes the "filling in" of the voids, the reoxidizing of the metallic particles, and the thickening of the thinner oxide regions, all resulting in a densified sputtered/anodized oxide.

The anodization of sputtered oxide is somewhat different from standard anodization of pure metal. Fig. 3 depicts a typical anodization behavior of sputtered tantalum oxide to form the 1200-Å-thick sputtered/anodized tantalum oxide, showing the anodization voltage V and current density J versus anodization time t. The RF sputtered tantalum oxide of 1100 Å in thickness was anodized by a standard constant-current anodization scheme. As the anodization cell was turned on, the anodization voltage rose rapidly, showing a small leakage current. The time rate of voltage increase dV/dt was much faster than that for the standard anodization of pure tantalum. When the anodization voltage approached the preset voltage, the anodic current rose abruptly up to the preset current by converting the sputtered oxide into a densified sputtered/anodized oxide. At this moment the conversion of the oxide structure could be perceived from the appearance of a more transparent sputtered/anodized oxide. As the anodization voltage reached the preset voltage of 75 V, which corresponds to the forming voltage for 1200-Å-thick anodic oxide, the anodization was changed to a constant-voltage mode, which continued for at least 10 min while the anodization current decayed. The key criterion for an effective reoxidation is that the anodization should proceed up to the voltage that achieves a large anodic current. Since the anodic current at the initial phase is only

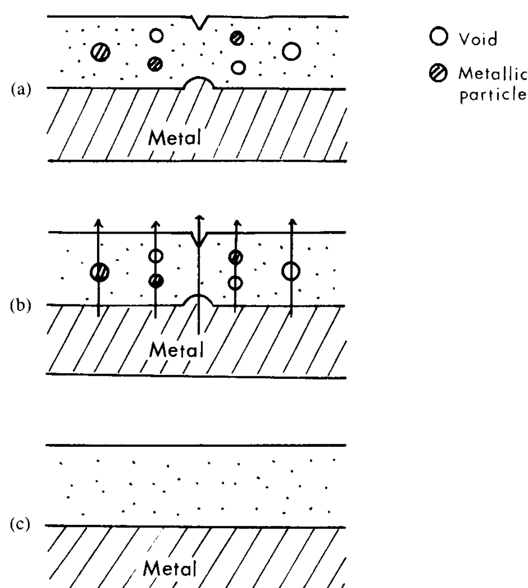

Fig. 2. Physical mechanism for oxide densification by the sputtered/anodized process. (a) Sputtered oxide. (b) Anodization. (c) Densified sputtered/anodized oxide.

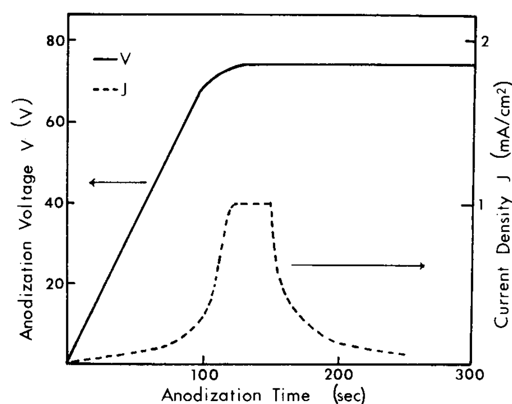

Fig. 3. Typical V–t and J–t curves for 1200-Å-thick sputtered/anodized oxide.

the electrical leakage current, structural conversion does not occur if the anodization is interrupted before the appearance of ionic movement as initiated by the large anodic current. During the densification of the oxide, the Ta underlay works as a seed layer for sealing the weak spots. In sputtered/anodized oxides, thin pure anodic oxide layers are grown at the Ta–oxide and oxide–electrolyte interfaces. The additional thickness due to the thin pure anodic layers slightly increases with increasing duration of the full constant-current mode anodization.

IV. Results and Discussion

A. Electrical Properties

The dielectric constant for each type of tantalum oxide at the chosen oxide thickness was calculated from the ca-

pacitance and the oxide thickness. The dielectric constant of the anodized oxide is in the range of 21–23, where thinner oxides exhibit the lower values. The dielectric constant of the sputtered oxide is about 22 or below and shows little thickness dependence. The dielectric constant of the sputtered/anodized oxide is in the range of 22–22.5, also showing little thickness dependence.

1) Dissipation Factor: The dissipation factor is an indication of the structural imperfections associated with defects in an oxide film. The dissipation factor versus oxide thickness plots of the tantalum oxide capacitors measured at 10 kHz are shown in Fig. 4. The anodized oxide exhibits a much higher dissipation factor than do the other oxides. The dissipation factor of the anodized oxide increases markedly as the oxide thickness decreases, which implies that the large amount of interfacial defects is mainly responsible for the increase in dissipation factor due to structural inhomogeneity. The sputtered oxide exhibits lower dissipation factors than the anodized oxide. The sputtered/anodized oxide shows the lowest dissipation factor with little thickness dependence among the three types of oxides. This indicates that the sputtered/anodized oxide has less defects such as voids, oxygen vacancies, and metallic particles than do the other oxides. It is found that the dissipation factor is correlated with other electrical properties. Tantalum oxide with a high dissipation factor exhibits a low breakdown field caused by large leakage currents.

2) Electrical Breakdown: Electrical breakdowns were characterized statistically by applying a ramped voltage to the capacitors at a ramp rate of 0.5–1.0 V/s and observing the leakage current through the oxide. As the electric field increases, the leakage current increases sharply at a critical electric field by showing a deviation from the normal exponentiallike increase of the leakage current prior to the occurrence of destructive breakdown. This critical electric field was defined as the breakdown field of the tantalum oxide capacitor. The breakdown field for tantalum oxide is dependent on the oxide thickness [10]. The breakdown field for the sputtered oxide under positive voltage on the Ta electrode is about 2.5 MV/cm or below, which is relatively independent of the oxide thickness. The breakdown field for the anodized oxide under positive voltage on the tantalum electrode is about 3.6 MV/cm in oxide thicknesses above 1200 Å, and it decreases dramatically when the oxide thickness decreases. The sputtered/anodized oxide under positive voltage on the Ta electrode shows much higher breakdown fields than do the other oxides. The breakdown field for the sputtered/anodized oxide is between 6.2 and 6.5 MV/cm and shows little thickness dependence. This is a great improvement in the dielectric strength of tantalum oxide films compared with conventional tantalum oxide films having low dielectric strength. The anodic oxidation of the sputtered tantalum oxide results in a great increase in breakdown field for the tantalum oxide film. It indicates that the subsequent anodic oxidation of the sputtered tantalum oxide results in a "filling in" of the micropores as well as a more complete oxidation of the weakly oxidized spots in the sputtered oxide film.

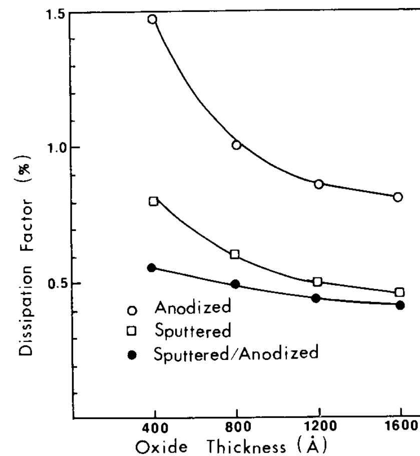

Fig. 4. Thickness dependence of dissipation factor of tantalum oxide capacitors measured at 10 kHz.

The breakdown distributions for the three types of 1200-Å-thick tantalum oxide capacitors under positive voltage on the Ta electrodes are shown in Figs. 5–7. For each type of oxide, 50–80 capacitors are tested. The anodized oxide shows a wide spread of breakdown fields, with a peak at the electric field between 3.5 and 4 MV/cm. The anodized oxide exhibits a low-field tail caused by defect-related breakdowns. The sputtered oxide also exhibits a wide spread of breakdown fields by showing defect-related breakdowns at low electric fields. In contrast to these results, the breakdown distribution for the sputtered/anodized tantalum oxide capacitors is very narrow, and most of the breakdowns occur at high electric fields of 6–7 MV/cm. The narrow breakdown distribution in the sputtered/anodized oxide suggests that the weak spots existing in the initial sputtered oxide are sealed after anodic reoxidation.

3) Charge Storage Capacity: Maximum charge storage capacity per unit area, i.e., $Q = CV_{BD}$, is calculated by multiplying the capacitance C with the statistically measured average breakdown voltage V_{BD} of tantalum oxide capacitors. The plots of the thickness dependence of the maximum anodic charge storage capacity, i.e., $Q^+ = CV_{BD}^+$, for the tantalum oxide capacitors under positive voltage on the Ta electrodes are shown in Fig. 8. The anodized oxide with an oxide thickness above 800 Å exhibits higher storage capacity than the sputtered oxide. However, the storage capacity for the anodized oxide capacitor decreases dramatically with decreasing oxide thickness because of a decrease in breakdown field. The charge storage capacity for the sputtered oxide is relatively independent of the oxide thickness. The sputtered/anodized oxide capacitor has much higher storage capacity than the other conventional oxide capacitors. The charge storage capacity for the sputtered/anodized tantalum oxide is in the range of 11.5–12 $\mu C/cm^2$ and shows

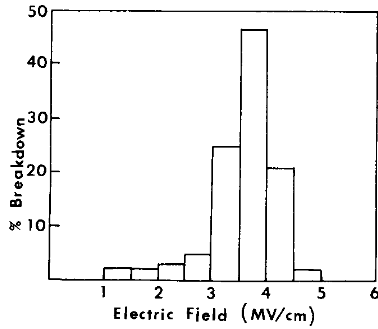

Fig. 5. Breakdown distribution for 1200-Å-thick anodized tantalum oxide capacitors.

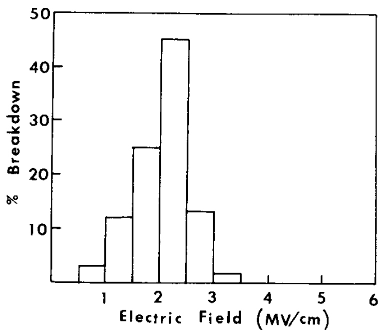

Fig. 6. Breakdown distribution for 1200-Å-thick sputtered tantalum oxide capacitors.

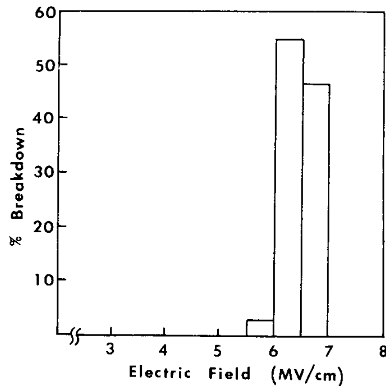

Fig. 7. Breakdown distribution for 1200-Å-thick sputtered/anodized tantalum oxide capacitors.

little thickness dependence. A comparison between the storage capacity for the sputtered/anodized tantalum oxide and previously reported storage capacities for SiO_2 and Si_3N_4 [11] suggests that the sputtered/anodized tantalum oxide can provide much higher charge storage capacity than SiO_2 and Si_3N_4.

The cathodic charge storage capacity, i.e., $Q^- = CV_{BD}^-$, is calculated after measuring the cathodic breakdown voltage V_{BD}^- of tantalum oxide capacitors by apply-

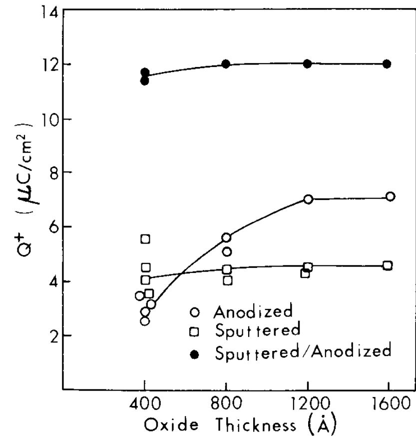

Fig. 8. Thickness dependence of maximum charge storage capacity of tantalum oxide capacitors.

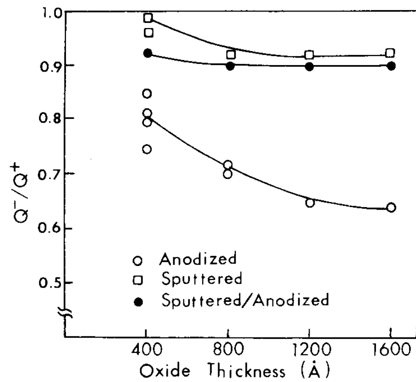

Fig. 9. Asymmetric charge storage ratio of tantalum oxide capacitors.

ing positive voltage to the Al electrodes. Plots of the asymmetric charge storage ratio Q^-/Q^+ versus oxide thickness are shown in Fig. 9. The ratios for the sputtered and the sputtered/anodized oxide capacitors are relatively symmetric. The charge storage ratio Q^-/Q^+ for the anodized oxide capacitor is between 0.65 and 0.7 for oxide thicknesses above 1200 Å. The increase of Q^-/Q^+ for the anodized oxide capacitor with decreasing oxide thickness is attributed to a decrease of V_{BD}^+. These results suggest that the sputtered/anodized tantalum oxide is more useful for applicatons to high-density memory storage capacitors than the other tantalum oxides.

4) Leakage Current: Leakage currents for both polarities of applied voltage were measured by applying a ramped voltage. The anodic leakage currents for the 1200-Å tantalum oxide capacitors under positive voltage on the Ta electrodes are shown in Fig. 10. The distinguishable phenomenon from the current versus field (I-E) characteristics is that the anodized oxide around the breakdown field exhibits much larger current levels than do the other oxides. This result suggests that the anodized oxide is capable of passing large leakage currents without showing

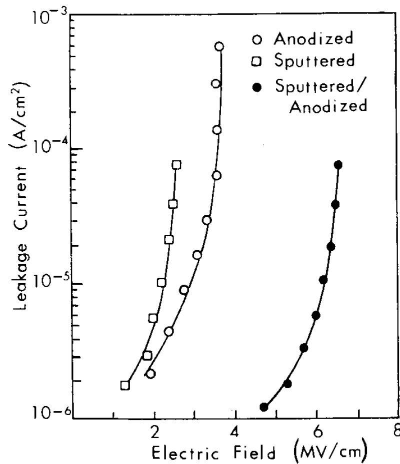

Fig. 10. Anodic leakage current versus electric field for 1200-Å-thick tantalum oxide capacitors.

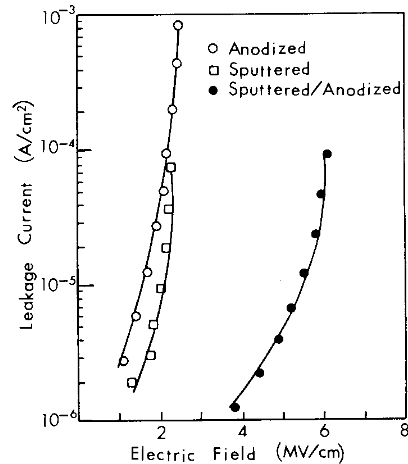

Fig. 11. Cathodic leakage current versus electric field for 1200-Å-thick tantalum oxide capacitors.

destructive breakdown. For the anodized and the sputtered oxides, the measured leakage currents rise very rapidly at low applied voltage. In contrast, the onset of large leakage currents for the sputtered/anodized oxide occurs at a much higher electric field. The cathodic leakage currents for the 1200-Å tantalum oxide capacitors under positive voltage on the Al electrodes are shown in Fig. 11. Evidently, the *I–E* curve of the anodized oxide is shifted toward a lower electric field compared with the anodic *I–E* curve, which is an evidence of the asymmetric conduction behavior of anodized tantalum oxide. The cathodic *I–E* curve for sputtered/anodized tantalum oxide compared with the corresponding anodic *I–E* curve is slightly shifted toward a lower electric field.

B. Physical Properties

X-ray photoelectron spectrocopy (XPS) analysis was used to study the physical properties of the three types of oxides. The Ta 4*f* spectra corrected for charge shifting by using the carbon peak at 284.6 eV as a reference binding energy are shown in Fig. 12. The Ta 4*f* spectra for the sputtered and anodized oxides show binding energy peaks at 26.5 and 26.8 eV, respectively, indicating weakly bound oxide states. The Ta 4*f* spectrum for the sputtered/anodized oxide shows a peak at 28.6 eV, which is significantly higher than that of the anodized or the sputtered oxide. The shift toward a higher binding energy in the sputtered/anodized oxide compared with the sputtered oxide can be interpreted as a chemical shift of core electrons in the oxide due to the two-step oxidation, which causes strong binding between metal and oxygen atoms. This indicates the more complete oxidation of the sputtered/anodized oxide film which leads to its superior dielectric properties.

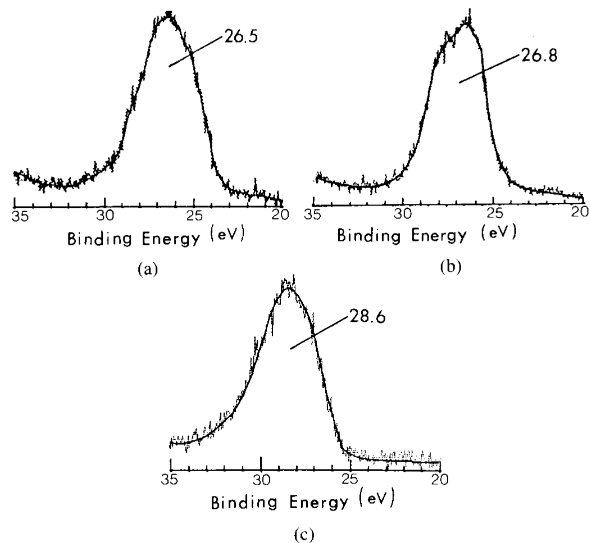

Fig. 12. Tantalum 4*f* XPS spectra for tantalum oxides. (a) Anodized. (b) Sputtered. (c) Sputtered/anodized.

C. Reliability

1) Interface Charge Trapping: Charge trapping phenomena at the metal–oxide interface have been measured to evaluate the oxide reliability. When a repetitively ramped voltage is applied to a capacitor, the *I–V* curve corresponding to the second voltage ramp is shifted due to interface trapping [12]. Fig. 13 shows sequential-ramp *I–V* curves for the anodized tantalum oxide obtained by applying positive voltage to the Ta electrode. The upper curve is the initial-ramp *I–V* curve, and the lower the second-ramp *I–V* curve after interface charge trapping. A large shift of the second-ramp *I–V* curve from the initial *I–V* curve indicates significant charge trapping at the metal–oxide interface. The second-ramp *I–V* curve shows a decrease in leakage current caused by electron trapping. After filling of the traps, the slope of the second *I–V* curve is larger than that of the initial *I–V* curve. The filling of

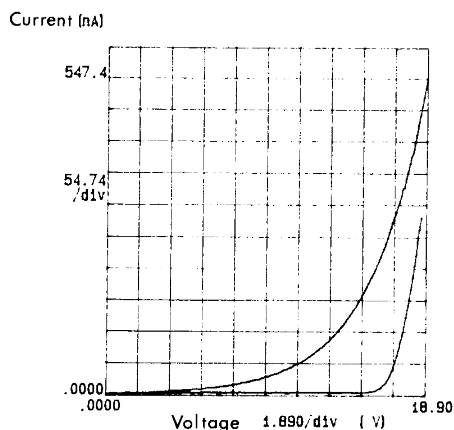

Fig. 13. Sequential-ramp $I-V$ curves for 500-Å-thick anodized tantalum oxide films with Ta positive. Upper curve—initial-ramp $I-V$; lower curve—second-ramp $I-V$.

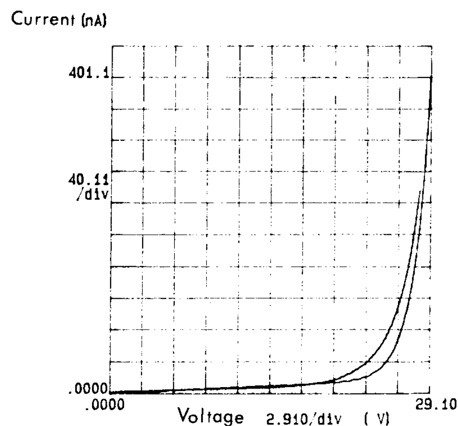

Fig. 14. Sequential-ramp $I-V$ curves for 500-Å-thick sputtered/anodized tantalum oxide films with Ta positive. Upper curve—initial-ramp $I-V$; lower curve—second-ramp $I-V$.

traps leads to a larger leakage current at a given electric field than the initial leakage current at the same electric field. This can be observed from the extension of the second $I-V$ curve, which exceeds the initial $I-V$ curve.

The sequential-ramp $I-V$ curves in the sputtered/anodized tantalum oxide are plottted in Fig. 14. The second-ramp $I-V$ curve (lower curve) shows little shift from the initial curve, which indicates less interface trapping compared to the anodized tantalum oxide. Similar sequential-ramp $I-V$ curves for sputtered tantalum oxide show different behavior. The second $I-V$ curve for the sputtered oxide shifts toward a lower voltage from the initial $I-V$ curve. It is considered that the opposite shift is associated with fast states at the metal-oxide interface. When the third voltage ramp is applied, the third $I-V$ curve shifts only slightly from the second-ramp $I-V$ curve. The large shift of the second $I-V$ curve toward a lower voltage is caused by detrapping of electrons that were trapped at low energy levels during the first voltage ramp or generation of positive charges [15] due to oxygen vacancies near the metal-oxide interface.

2) Charge Trapping under Current Stress: The behavior of charge trapping at the near interface or in the oxide bulk has been obtained by measuring voltage versus time ($V-t$) characteristics of tantalum oxide under constant-current stress. The normalized voltage versus time curves for the three types of tantalum oxide capacitors under constant-current stress on the Ta electrodes are plotted in Fig. 15. The rapid increase in voltage before reaching the peak voltage V_p corresponds to the transient associated with the fast interface trapping [14] and a relaxation mechanism. The magnitude of V_p, which is the voltage required to maintain the constant current, is determined by the extent of leakage current in the oxide. In the actual measurements, the sputtered/anodized oxide showed much higher electrode voltage than the sputtered or anodized oxides. This implies that the sputtered/anodized oxide has a higher dielectric resistance to electron transport than do the other

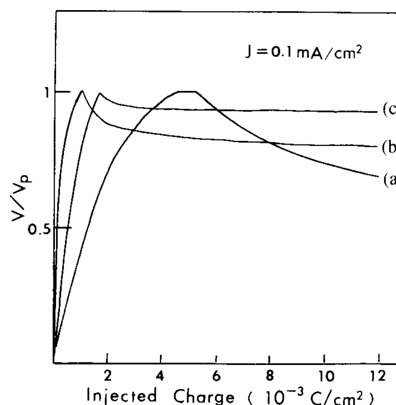

Fig. 15. V/V_p versus injected charge for 400-Å-thick tantalum oxide films under current stress on Ta electrodes. (a) Anodized. (b) Sputtered. (c) Sputtered/anodized.

oxides. The decrease in electrode voltage V, after reaching V_p, is due to slow trapping near the metal-oxide interface or in the oxide bulk. The relative ratio of V to V_p is an indication of the amount of trapped electron charges or positive charges in the oxide. The sputtered/anodized oxide shows a smaller decrease in V/V_p than the sputtered oxide, which implies less degradation of the oxide. The anodic oxide shows a longer transient associated with the dominant slow trapping [14] caused by a conductivity gradient at the metal-oxide interface. It is obvious that the sputtered/anodized tantalum oxide with little charge trapping and high dielectric resistance is the best reliable oxide among the three types of oxides.

3) TDDB Properties: Time-dependent dielectric breakdown (TDDB) for the tantalum oxides has been measured by applying either constant current or positive voltage to the Ta electrodes. The time to breakdown t_{BD} for each type of oxide is estimated by measuring 50-percent cumulative failures for 30–50 capacitors from two

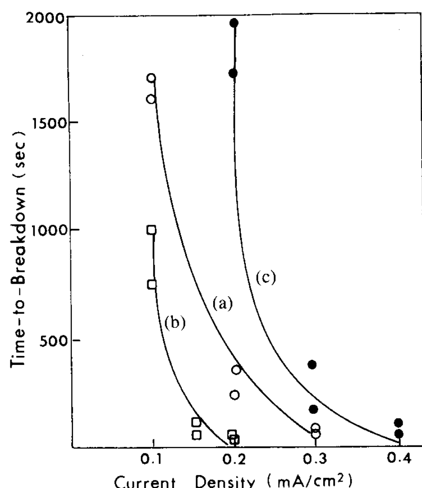

Fig. 16. Time to breakdown t_{BD} of 50% failures for 800-Å-thick tantalum oxide films under current stress on Ta electrodes. (a) Anodized. (b) Sputtered. (c) Sputtered/anodized.

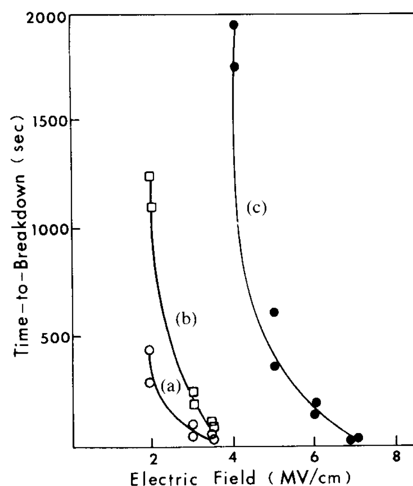

Fig. 17. Time to breakdown t_{BD} of 50% failures for 800-Å-thick tantalum oxide films under voltage stress on Ta electrodes. (a) Anodized. (b) Sputtered. (c) Sputtered/anodized.

lots of simultaneously processed wafers. As the tantalum oxide was stressed by either current or voltage, a rapid decrease of voltage or a sharp current spike prior to destructive breakdown was observed from instabilities in the V–t or I–t curve during the time-domain measurements. The time showing instable voltage or current was defined as the time to breakdown. The TDDB properties for the three types of 800-Å-thick tantalum oxides under constant-current stress are shown in Fig. 16. The anodized oxide shows better TDDB properties than the sputtered oxide. The sputtered/anodized oxide shows much superior TDDB properties than do the other oxides.

Fig. 17 shows the voltage-stressed TDDB properties for the 800-Å-thick tantalum oxides. In contrast to the current-stressed TDDB properties, the anodized oxide shows TDDB properties inferior to the sputtered oxide. The sputtered/anodized oxide also shows the best TDDB properties among the three types of oxides. A comparison of Figs. 16 and 17 suggests that the anodized oxide is less degraded under current stress but more degraded under voltage stress compared with the sputtered oxide. It is found that the anodized oxide is a leaky insulator that is capable of passing large leakage current through imperfect dielectric spots due to defects. Therefore the anodized oxide is less degraded under current stress than the sputtered oxide because the imperfect dielectric spots are main paths for large leakage currents. From the TDDB measurements it is apparent that the sputtered/anodized oxide is the most promising oxide in terms of long-term reliability.

V. Conclusions

Reliable high-performance tantalum oxide capacitors have been developed by a novel reoxidation scheme. The two-step oxidized sputtered/anodized tantalum oxide capacitors have been shown to be quite useful for high-density VLSI memory storage capacitor applications because of the significantly higher breakdown field than the other tantalum oxide capacitors prepared by either anodization or sputtering alone. The superior properties of the sputtered/anodized tantalum oxides are achieved by anodically reoxidizing the RF sputtered tantalum oxides to densify the oxide structure. The oxide densification by the novel two-step oxidation process results in a decrease in the dissipation factor, less spread of breakdown distribution, an increase in storage capacity, and a decrease in leakage current in the sputtered/anodized tantalum oxide films. XPS analysis has shown that the sputtered/anodized tantalum oxide has a more completely oxidized structure. The sputtered/anodized tantalium oxide films with less charge trapping and better TDDB properties than the other conventional tantalum oxides are highly desirable for applications to DRAM storage capacitors and other microelectronic devices.

References

[1] K. Ohta, K. Yamada, K. Shimizu, and Y. Tarui, "Quadruply self-aligned stacked high-capacitance RAM using Ta_2O_5 high-density VLSI dynamic memory," *IEEE Trans. Electron Devices*, vol. ED-29, pp. 368–376, 1982.

[2] Y. Nishioka *et al.*, "Ultra-thin Ta_2O_5 dielectric film for high-speed bipolar memories," *IEEE Trans. Electron Devices*, vol. ED-34, pp. 1957–1962, 1987.

[3] N. N. Axelrod and N. Schwartz, "Asymmetric conduction in thin film tantalum/tantalum oxide/metal structures: interstitial and substitutional impurity effects and direct detection of flaw breakdown," *J. Electrochem Soc.*, vol. 116, pp. 460–465, 1969.

[4] N. W. Silcox and L. I. Maissel, "Some factors controlling gross leakage currents in sputtered tantalum-film capacitors," *J. Electrochem. Soc.*, vol. 109, pp. 1151–1154, 1962.

[5] M. E. Elta, A. Chu, L. J. Mahoney, R. T. Cerretani, and W. E. Courtney, "Tantalum oxide capacitors for GaAs monolithic integrated circuits," *IEEE Electron Device Lett.*, vol. EDL-3, pp. 127–129, 1982.

[6] G. S. Oehrlein, "Oxidation temperature dependence of the dc electrical conduction characteristics and dielectric strength of thin Ta_2O_5 films of silicon," *J. Appl. Phys.*, vol. 59, pp. 1587–1595, 1986.

[7] S. Kimula, Y. Nishioka, A. Shintani, and K. Mukai, "Leakage-current increase in amorphous Ta_2O_5 films due to pinhole growth during annealing below 600°C," *J. Electrochem. Soc.*, vol. 130, pp. 2414–2418, 1983.
[8] S. Robert, J. Ryan, and L. Nesbit, "Selective studies of crystalline Ta_2O_5 films," *J. Electrochem. Soc.*, vol. 133, pp. 1405–1410, 1986.
[9] S. G. Byeon and Y. Tzeng, "Improved oxide properties by anodization of aluminum films with thin sputtered aluminum oxide overlays," *J. Electrochem. Soc.*, vol. 135, pp. 2452–2458, 1988.
[10] S. G. Byeon and Y. Tzeng, "High performance sputtered/anodized tantalum oxide capacitors," in *IEDM Tech. Dig.*, 1988, pp. 722–725.
[11] W. P. Noble and W. W. Walker, "Fundamental limitations on DRAM storage capacitors," *IEEE Circuits Devices Mag.*, vol. 1, pp. 45–51, 1985.
[12] P. Solomon, "High-field electron trapping in SiO_2," *J. Appl. Phys.*, vol. 48, pp. 3843–3849, 1977.
[13] E. Harari, "Dielectric breakdown in electrically stressed thin films of thermal SiO_2," *J. Appl. Phys.*, vol. 49, pp. 2478–2489, 1978.
[14] S. K. Lai and D. R. Young, "Effects of avalanche injection of electrons into silicon dioxide-generation of fast and slow states," *J. Appl. Phys.*, vol. 52, pp. 6231–6240, 1981.

*

Sang Gi Byeon received the B.S. degree in electronic engineering from Yonsei University, Seoul, Korea, in 1974 and the M.E. degrees in electronic engineering from Yonsei University in 1978 and the University of Florida in 1986. Since 1986 he has been working toward the Ph.D. degree at Auburn University, Auburn, AL.

From 1978 to 1984 he was with the Hong-Loong Machinery Corporation, Korea, where he was engaged in the design of analog amplifiers and digital logic circuits for communication systems as a Senior Research Engineer. His current research interests are thin oxide devices, VLSI memories, and process development in microelectronic fabrication.

*

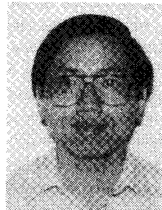

Yonhua Tzeng (M'84) was born in Chia-Yi, Taiwan, Republic of China, on February 2, 1955. He received the B.S. degree in 1977 from the National Taiwan University, Taipei, and the M.S. and Ph.D. degrees in 1981 and 1983, respectively, from Texas Tech University, Lubbock, TX, all in electrical engineering.

He joined Auburn University, Auburn, AL, in 1983 as an Assistant Professor of Electrical Engineering, was promoted to the rank of Associate Professor in 1988, and was awarded the Alumni Professorship in 1989. Since 1979 he has been working on plasma kinetics and the processing of electronic materials, including silicon, GaAs, high-temperature superconductor, diamond thin films, and dielectric materials. He is currently in charge of the Plasma Processing and Electronic Materials Laboratory in the Alabama Microelectronics Science and Technology Center. He has published a large number of papers in his areas of research.

Dr. Tzeng is a member of the Phi Kappa Phi, the IEEE Electron Devices Society, the American Vacuum Society, and the Electrochemical Society.